

# MEMS Sensor Development for In-Situ Quantification of Toxic Metals in Sediment

FINAL REPORT  
December 2022

Mehdi Javanmard  
Associate Professor

Submitted by:

Robert Miskewitz  
Research Associate Professor

Rutgers University  
94 Brett Rd.  
Piscataway, NJ 08854

External Project Manager:

Ali Maher, Professor  
Rutgers University

In cooperation with

Rutgers, The State University of New Jersey  
And  
New Jersey Department of Transportation  
And  
U.S. Department of Transportation  
Federal Highway Administration

## **Disclaimer Statement**

The contents of this report reflect the views of the authors, who are responsible for the facts and the accuracy of the information presented herein. This document is disseminated under the sponsorship of the Department of Transportation, University Transportation Centers Program, in the interest of information exchange. The U.S. Government assumes no liability for the contents or use thereof.

The Center for Advanced Infrastructure and Transportation (CAIT) is a Regional UTC Consortium led by Rutgers, The State University. Members of the consortium are Atlantic Cape Community College, Columbia University, Cornell University, New Jersey Institute of Technology, Polytechnic University of Puerto Rico, Princeton University, Rowan University, SUNY - Farmingdale State College, and SUNY - University at Buffalo. The Center is funded by the U.S. Department of Transportation.

1. Report No. CAIT-UTC-REG7	2. Government Accession No.	3. Recipient's Catalog No.	
4. Title and Subtitle <b>MEMS Sensor Development for In-Situ Quantification of Toxic Metals in Sediment</b>		5. Report Date December 2022	
		6. Performing Organization Code CAIT/Rutgers University	
7. Author(s) Azam Gholizadeh ( <a href="https://orcid.org/0000-0002-6634-758X">https://orcid.org/0000-0002-6634-758X</a> ) Sakshi Sardar ( <a href="https://orcid.org/0000-0001-5527-0217">https://orcid.org/0000-0001-5527-0217</a> ) Kelly Francisco ( <a href="https://orcid.org/0000-0002-6393-2097">https://orcid.org/0000-0002-6393-2097</a> ) Mehdi Javanmard ( <a href="https://orcid.org/0000-0002-6297-392X">https://orcid.org/0000-0002-6297-392X</a> ) Robert Miskewitz ( <a href="https://orcid.org/0000-0002-7052-4702">https://orcid.org/0000-0002-7052-4702</a> )		8. Performing Organization Report No. CAIT-UTC-REG7	
		9. Performing Organization Name and Address Rutgers University 94 Brett Rd. Piscataway, NJ 08854	
12. Sponsoring Agency Name and Address Center for Advanced Infrastructure and Transportation Rutgers, The State University of New Jersey 100 Brett Road Piscataway, NJ 08854		11. Contract or Grant No. 69A3551847102	
		13. Type of Report and Period Covered Final Report 9/1/2018 – 9/30/2019	
15. Supplementary Notes U.S. Department of Transportation/OST-R 1200 New Jersey Avenue, SE Washington, DC 20590-0001		14. Sponsoring Agency Code	
16. Abstract In this project, we developed a novel, integrated on-chip sample-to-answer platform capable of detecting lead ions (Pb <sup>+2</sup> ) directly in sediment samples. As sediment is one of the main sources of hazardous heavy metals in aquatic ecosystems, rapid and real-time detection of heavy metals in sediment is crucial in the field of environmental monitoring. Electrochemical sensors can provide rapid detection capability, but in-situ measurement of heavy metals with such sensors has been limited by complicated pretreatment steps. To overcome this drawback, an integrated system was developed consisting of a porous matrix for purification and extraction of Pb <sup>+2</sup> onto a graphene oxide thin film that serves as an active sensing material. The integrated sensor with a 3D porous matrix was used as an in-situ platform to detect lead directly in complex sediment samples. The proposed electrochemical sensor has a detection limit of 4 ppb and a linear working range. The ability to directly detect lead in sediment samples with minimal pretreatment agents and time makes this system a promising solution for on-site monitoring of heavy metals in environmental samples. Although the current study focused on lead for platform validation, the proposed sensing platform can be further developed for the detection of a wide panel of toxic metals.			
17. Key Words Lead, toxic metals, MEMS, sensors		18. Distribution Statement	
19. Security Classification (of this report) Unclassified	20. Security Classification (of this page) Unclassified	21. No. of Pages 22	22. Price

## **Acknowledgments**

The authors would like to thank Masoud Janbaz for helping with sediment collection.

## Table of Contents

Description of Problem	p.6
Methodology	p. 8
Findings	p. 10
Conclusion	p. 18
Recommendations	p. 22

## List of Figures

Fig. 1. Image of compact electrochemical lead sensor. The schematic of set up design and SEM of cellulose sponge, scale bar is 200  $\mu\text{m}$ .

Fig. 2. (A,B) SEM image of GO thin film on gold electrode surface, (C,D) 2 and 3D Atomic force microscopy images on glass slide. (E) Raman spectrum of GO, and (F) rGO image.

Fig. 3. (A, B) Differential pulse voltammograms obtained for different GO and rGO concentration electrodes respectively. DPV performed from  $-0.9$  to  $-0.2$  V, with step size 10 and pulse size 50 mV in 10 ppm lead in 0.1 M acetate buffer (pH 5). (C) Cyclic voltammograms of different GO concentrations electrodes in 5 mM  $\text{K}_3\text{Fe}(\text{CN})_6$  in 0.1 M KCl. Scan rate is 20  $\text{mVs}^{-1}$ . (D) Electrochemical impedance curves in 5 mM  $\text{K}_3\text{Fe}(\text{CN})_6/\text{K}_4\text{Fe}(\text{CN})_6$ , 0.1 M KCl. The spectra were taken at 0.1 Hz to 1 MHz, 0.115 V vs Ag/AgCl.

Fig. 4. (A, B) Square wave anodic stripping voltammograms of different pulse amplitude, frequency, (C, D) accumulation time and accumulation voltage respectively. Lead concentration used was 20 ppm in 0.1 acetate buffer (pH 5).

Fig. 5. (A, B) Square wave anodic stripping voltammograms of different range of lead standard solution in acetate buffer (0-20 ppm). Pulse size is 50 mV, frequency 20 Hz, accumulation time 240 s. (C, D) Calibration curves for different concentration range of lead standard solutions.

Fig. 6. (A) Solution of sediment in nitric acid before and after filtration. (B) Effect of concentration of nitric acid using ultrasound digestion in 60 degrees a) digested in 0.1 M nitric acid, b) 0.2 M nitric acid. c) blank buffer solution 0.2 M nitric acid/acetate buffer, d) 0.3 M nitric acid (C) SWASV peaks for different concentration of lead standard solution in 1:1 nitric acid and acetate buffer. (D) SWASV peaks for a) 0.1 M nitric acid/acetate buffer blank, b) digested lead in 0.1 M nitric acid/acetate buffer.

Fig. 7. (A) Column based pretreatment set up, (B) SWASV response of column based compact electrochemical lead sensor, (C) Calibration curve for (1:1) nitric acid: acetate after baseline correction, (D) comparing results for different pretreatment approaches based on calibration curve.

## DESCRIPTION OF THE PROBLEM

One of the most dominant heavy metals present in the environment is lead as it is widely used in building materials, lead paints, and lead-acid batteries. As a result of its abundance in the environment, particularly in natural water sources and drinking water, lead poisoning has resulted in many public health epidemics. Lead and other toxic particulates in natural water often settle into the sediment, which is resuspended into the water column due to storms and transit of boats and vessels. The high concentration of lead in sediment (reported in the range of  $\text{mg kg}^{-1}$  [1]) poses risks to aquatic organisms and becomes a serious public health problem when it gets reentrained into the water column. Lead can damage the human nervous (especially in children), respiratory, and reproductive systems [2]. Hence, the ability to rapidly screen sediment samples for lead is necessary to identify hot-spots of contaminated areas where remediation is necessary, thus minimizing the risk of re-suspension into natural water sources. To meet this requirement, there is a need for automated, portable, ultra-compact sensing devices capable of qualitatively identifying toxic metals directly in complex environmental samples without the need for sample handling and preparation. A variety of measurement methods have been developed to assess the extent of lead contamination. These methods include atomic absorption spectroscopy [3]–[6], inductive coupled plasma mass spectroscopy [7], [8], optical. [9], [10] and electrochemical methods based on ion selective electrodes [11], [12] and stripping voltammetry. [14]–[17]. Among these, the high speed, high sensitivity and portability of electrochemical-stripping voltammetry makes it a promising method for tools capable of field measurements. Stripping voltammetry works well in purified buffers, however, to date there have been no reports of electrochemical platforms capable of direct measurement of lead in sediment sample.

Electrochemical based sensors utilize a variety of electrode surface modifications for increasing sensitivity of lead detection. One example involves the reaction between tin and bismuth with lead and incorporation of these materials on the surface of the electrodes [18], [19]. A variety of other metal nanoparticles have been used, with the aim of increasing the surface area. [20], [21]. Other methods are based on using DNA enzymes [22], [23]. Additionally, graphene-based nanomaterials are another potential class of materials for electrode surface capable of sensitive lead detection [24]–[27], due to their extraordinary electronic transport properties, large surface area, higher cathodic window (avoiding reduction of hydrogen) and high electro-catalytic activities. Among them, graphene oxide, prepared through extensive chemical exfoliation of graphite flakes, has oxygen containing functional

groups such as hydroxy, carboxy, epoxy, ether, diol and ketone, which are active sites for adsorbing heavy metals such as lead. [19], [28].

Multiple methods are available that allow for relatively easy deposition of graphene oxide (GO) thin films on top of electrode surfaces. These methods include drop casting [24], [29], dip coating [29], Langmuir-Blodgett based deposition [30], transfer via vacuum filtration [31], and spin coating [33]–[35]. The method used for deposition of GO is very important to control surface morphology, film uniformity, thickness and surface coverage. Among these methods, dip coating and drop casting often result in non-uniform deposition due to aggregation of GO sheets. In addition, the drop casting of a GO suspension usually results in weak adhesion to electrode substrate. The rapid evaporation of the solvent during spin coating allows a more uniform surface with minimal wrinkling and increases the adhesion between the GO thin film and the electrode surface, which is critical during electrochemical reduction of GO.

Screen printed electrodes (SPE) have great utility as a disposable device, owing to a low cost of manufacture. SPEs can be used for point-of-use testing in various applications from industrial process monitoring to environmental monitoring and food testing. Combining screen-printed electrodes with stripping voltammetry provides a promising solution for detection of heavy metals such as lead [36]–[38]. Various lead sensors have already been developed using SPEs. One example is disposable bismuth oxide modified SPE for detection of lead in the range of 20–300 ppb with a detection limit of 8 ppb. [38]. Other studies have shown that SPEs modified by gold films displayed very highly linear behavior for lead concentrations between 2–16 ppb and a low detection limit of 0.5 ppb [39].

The key challenge to utilizing electrochemical methods at point-of-use for detecting heavy metals in complex matrices such as sediment, food and soil is the requirement to perform a separate pretreatment step for extraction of ions and purification of the sample [41]–[43]. For lead, the ion extraction step is essential to convert all various chemical forms of lead to  $Pb^{2+}$  so that they can participate in the electrochemical reaction.

## **APPROACH**

In this work, we present an ultra-compact sediment pretreatment module combined with a highly sensitive electrochemical graphene oxide sensor to detect lead in untreated sediment samples obtained directly from the

environment. Our sediment pre-treatment module consists of a cellulose sponge, which serves as a membrane between the sediment and the active site of the sensor. Sponges have previously demonstrated significant ability to adsorb oil contamination [43], making them a suitable choice of material as a porous membrane. The porous membrane adsorbs the analyte from the sediment, preventing direct contact between solid sediment and the active graphene oxide site. Lead ions easily penetrate through the cellulose sponge membrane and a pure solution reaches the graphene oxide surface. As an additional benefit, this set up minimizes the required acidic pretreatment to microliter levels.

In the present study, we selectively spin-coated a uniform layer of GO onto a screen-printed gold working electrode and optimized the performance of the sensor over a wide range of parameters. Gold screen-printed electrodes were chosen as the working electrode for the deposition of GO because they have a high conductivity and exhibit excellent performance of stripping voltammetry [45]–[47]. The surface morphology and chemical characterization of the GO film was analyzed using scanning electron microscopy (SEM), atomic force microscopy (AFM) and Raman Spectroscopy. The analytical parameters affecting the sensor performance and the thin film fabrication were studied in terms of the concentration of GO solution during spin coating, the effect of GO reduction, the supporting electrolyte, and square wave anodic stripping voltammetry (SWASV) parameters such as deposition time, frequency, and pulse height. The reliability of the electrode in response to high concentrations of lead was also investigated to ensure the capacity of lead adsorption on the surface of the electrode. Furthermore, the effect of water extracted from sediment on the supporting electrolyte was investigated both with and without adding acetate buffer solution in the range of 0 ppb to 20 ppm lead standard. This was then used to quantify the amount of lead present in digested sediment samples that were collected from the environment.

## **METHODOLOGY**

### **A. Reagents and Instrumentation**

Pb (II) standard solution was prepared using lead nitrate stock standard solution in supporting electrolytes. GO solutions were prepared from standard stock solution of 2 mg mL<sup>-1</sup> (Sigma Aldrich, MO, USA). To avoid aggregation of GO sheets, each solution underwent ultrasonication and centrifugation



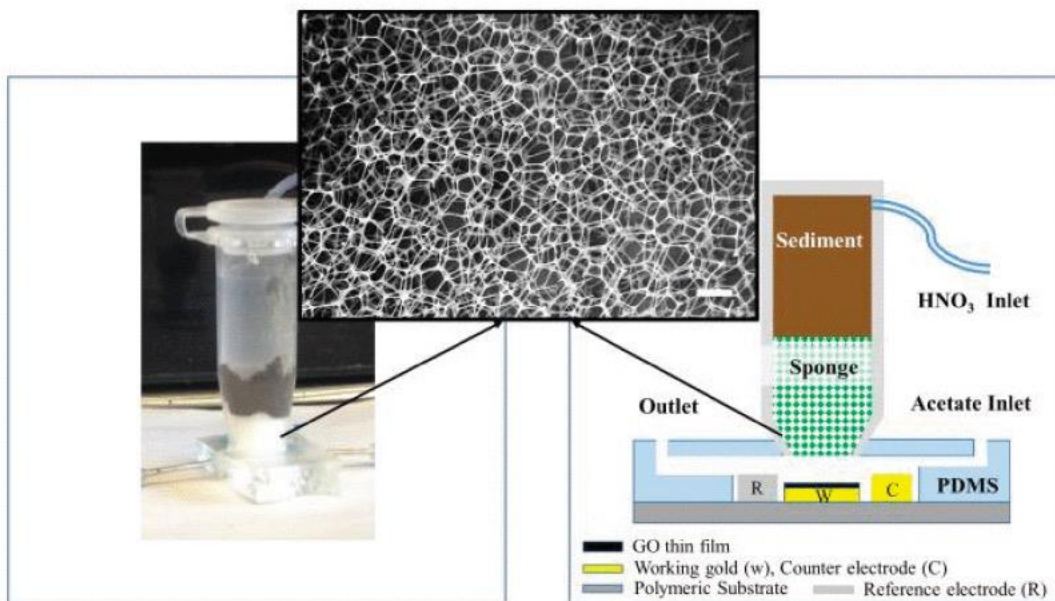
immediately prior to spin coating. A potentiostat (Gamry 600, Gamry Instruments, Pennsylvania, USA) was used to perform electrochemical measurements. Screen printed electrodes with gold working (5 mm) and counter electrodes and an Ag/AgCl reference electrode were purchased from USA Metrohm. All electrochemical experiments were conducted in ambient conditions, except for reduction of GO which underwent purging using high purity nitrogen. Ambient conditions were chosen to ensure that platform is fully compatible with field-use.

The morphology of graphene oxide was characterized using field-emission scanning electron microscopy (SEM) (Zeiss Leo Field Emission SEM, Carl Zeiss) and atomic force microscopy (AFM) (Digital Instruments Nanoscope IV). The atomic force microscope was operated in tapping mode using standard cantilevers with a spring constant of  $40 \text{ N m}^{-1}$  and a tip curvature of 10 nm. FT-Raman spectra (Horiba Jobin-Yvon Micro Raman Spectrometer, 532 nm excitation laser) were recorded to characterize graphene oxide substrates. The sediment sample was collected in the Arthur Kill at the mouth of Morse's Creek in Linden NJ. It was collected using a Smith Mack box corer lowered from a boat in a depth of approximately 6 feet of water. The sample consisted of a composite of the sediments from 0 to 25 cm below the sediment water interface.

## **B. Sensor Fabrication**

The compact sensor system developed herein comprises two main components, (i) a modified electrochemical sensor with GO, and (ii) a pretreatment column consisting of a cellulose sponge. The steps required to modify the gold working electrode with a spin coated layer of GO are shown in figure S1.

Figure 1 shows the schematic and an image of the fabricated compact sensor set up. The pretreatment column is assembled with a 5 mm polydimethylsiloxane (PDMS) layer. To connect the column to the sensor active site, an 8 mm hole is punched through the PDMS layer and an Eppendorf tube is used as the pretreatment column. The pretreatment column adheres on top of the hole with glue. A sponge (2 mm high) is located between the sediment sample and the hole inside the column. Syringe tips are used for inserting the required agents for pretreatment.



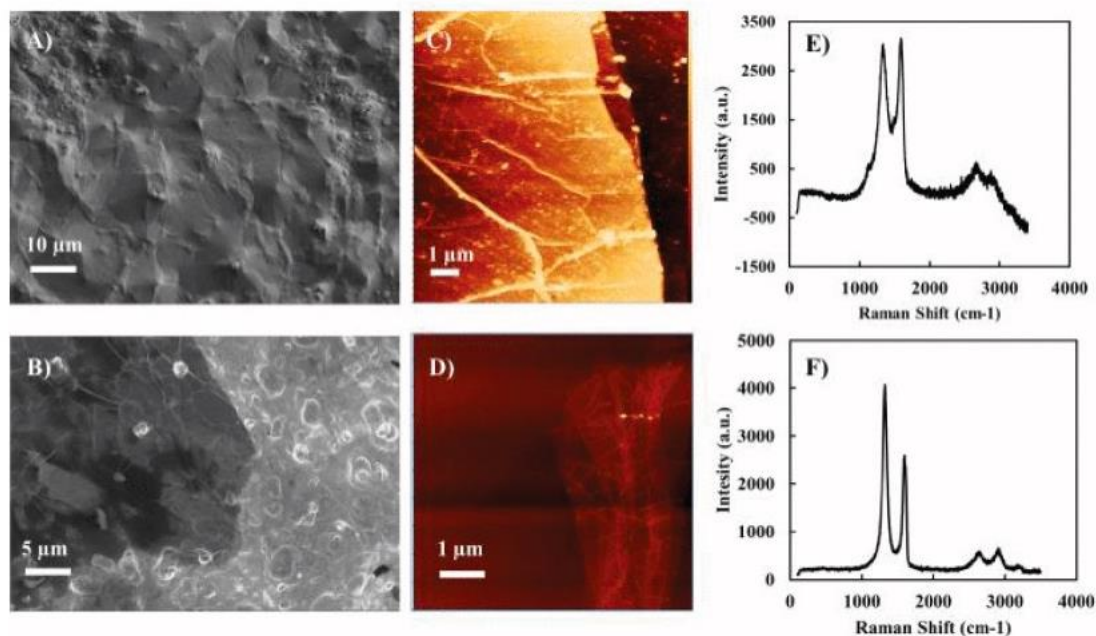
**Fig. 1.**

Image of compact electrochemical lead sensor. The schematic of set up design and SEM of cellulose sponge, scale bar is 200  $\mu\text{m}$  .

## FINDINGS

### A. GO Thin Film Characterization and Optimization

The morphology of the graphene oxide film was studied using AFM and SEM. Raman spectroscopy was used to determine the extent of reduction of the graphene oxide layer. Figure 2A,B show the SEM images taken from a spin-coated 2 mg mL<sup>-1</sup> graphene oxide layer on the surface of the working gold electrode. The figure illustrates that 50  $\mu\text{m}$  of a graphene oxide large sheet can form a uniform layer in most areas despite the roughness (micron scale features) of the gold electrode surface. In comparison to drop-casting, which is typically used in electrochemically modified electrodes, this method provides more reproducibility and enables formation of much larger areas of GO films without agglomeration. Figure 2C,D show two-dimensional AFM images of a graphene oxide flake with wrinkles. These wrinkles can be produced during vaporization of the solvent during spin coating. From the height profile, the film can be approximated to have a thickness of 1.5 nm, which is typical amount for GO sheet (figure S2).



**Fig. 2.**

(A, B) SEM image of GO thin film on gold electrode surface, (C, D) 2 and 3D Atomic force microscopy images on glass slide. (E) Raman spectrum of GO, and (F) rGO image.

This study tested and characterized both graphene oxide and reduced graphene oxide films to determine which performs better for the detection of lead. Both the extent of electrochemical reduction of the GO films and the quality of reduction were investigated using Raman spectroscopy. Figure 2E shows the Raman spectrum of graphene oxide and the electrochemically reduced film. The most important features in the Raman spectra for assessment of graphene oxide reduction are the G and D peaks. These peaks arise from vibration of  $sp^2$  carbon and appear around 1600 and 1340  $cm^{-1}$  respectively. The overtone of the D peak appearing around 2700  $cm^{-1}$  is called the 2D peak. Unlike mechanically exfoliated graphene, the GO 2D band usually has low intensity because it is more disordered. Therefore, the peaks that can be used to distinguish between GO and rGO are the G and D peaks and their ratio (Figure 2F). Also, the G peak of GO and rGO with respect to graphene and graphite gets shifted into higher frequencies (1600  $cm^{-1}$ ) because of defects in the film. This ratio exhibited a significant increase compared to GO (from 0.98 to 1.57). This shows restoration of  $sp^2$  carbon and a decrease in the average size of  $sp^2$  domains after electrochemical reduction of GO. The increased intensity of the 2D peak also suggests better graphitization [47]. In order to explore the activation of the modified working electrode, the electrochemical performance was evaluated using differential pulse voltammetry (DPV). Figure 3A and 3B show that an increase in concentration of spin coated GO solution increases the current intensity in response to 10 ppm of lead standard solution. Also, the current intensity from

GO electrodes is higher compared to that of rGO, likely because the interaction between oxygen functionalized groups with lead ions. The data suggest that among the different working electrodes fabricated, the spin coated GO film (concentration of  $2 \text{ mg mL}^{-1}$ ) exhibits the fastest electron transfer rate for lead ions.

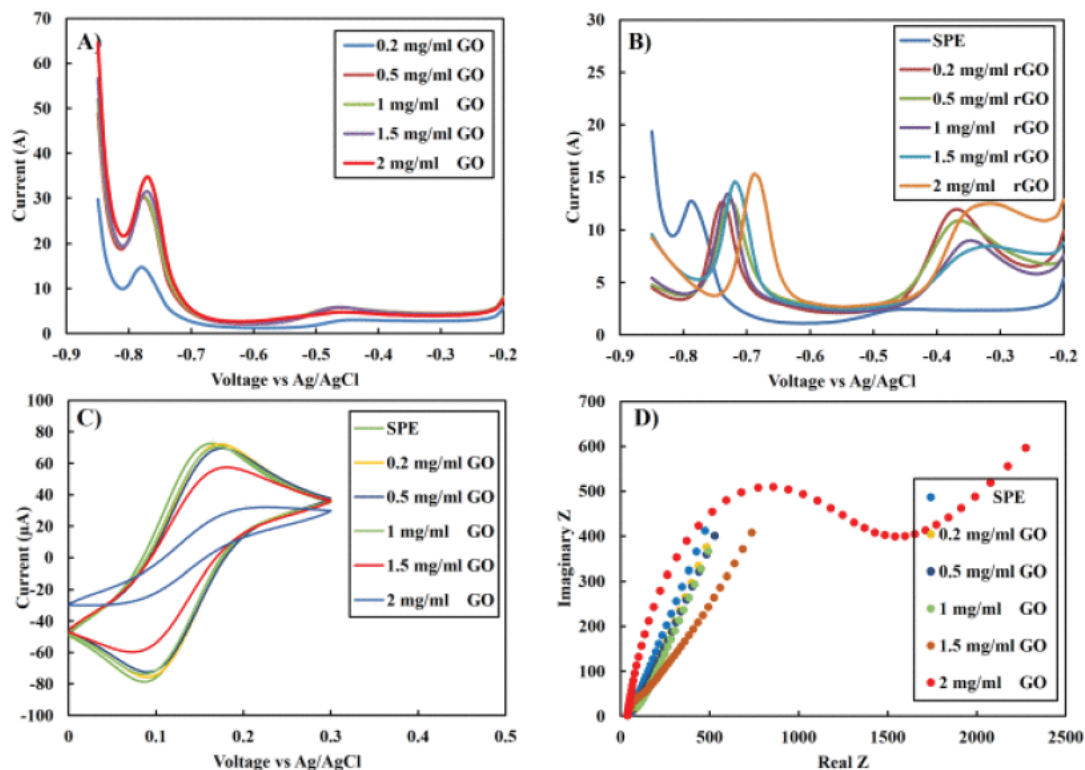


**Fig. 3.**

(A, B) Differential pulse voltammograms obtained for different GO and rGO concentration electrodes respectively. DPV performed from  $-0.9$  to  $-0.2$  V, with step size 10 and pulse size 50 mV in 10 ppm lead in 0.1 M acetate buffer (pH 5). (C) Cyclic voltammograms of different GO concentrations electrodes in 5 mM  $\text{K}_3\text{Fe}(\text{CN})_6$  in 0.1 M KCl. Scan rate is  $20 \text{ mVs}^{-1}$ . (D) Electrochemical impedance curves in 5 mM  $\text{K}_3\text{Fe}(\text{CN})_6/\text{K}_4\text{Fe}(\text{CN})_6$ , 0.1 M KCl. The spectra were taken at 0.1 Hz to 1 MHz, 0.115 V vs Ag/AgCl.

The electrode film was electrochemically characterized using an inner sphere redox probe, potassium ferrocyanide. Figure 3C shows representative data of cyclic voltammogram obtained for an unmodified gold SPE and various spin coated GO films. The gold SPE demonstrates a pair of well-defined redox peaks, with a peak-to-peak separation of 78 mV. The peak separation can be used to determine hetero-electron transfer (HET) rate. In the case of linear mass transfer,

smaller separation of the peaks indicates increasing reversibility and higher HET rate. Electrochemical characterization of the GO thin films exhibits an increasing peak separation with respect to the concentration of GO suspension. The peak separations for GO solution concentrations between 0.2–2 mg mL<sup>-1</sup> range from 82 to 176 mV. The electrochemical response of graphene based electrodes towards the ferrocyanide redox probe is influenced by the density of states near the Fermi level and more significantly by surface morphology and the presence of oxygenated species [48].

Electrochemical impedance spectroscopy (EIS) was used to further characterize the electrochemical performance of the device. Nyquist plots for the electrodes are shown in figure 3D. The shape of plot depends on the applied voltage. All impedances were biased to the redox voltage of ferrocyanide, which was 0.115 V. The charge transfer resistance (R<sub>ct</sub>) values, which are based on the real part of the impedance in EIS measurements, are in agreement with the cyclic voltammograms response. With increasing GO concentration, HET decreases and R<sub>ct</sub> increases. In addition, at 2 mg mL<sup>-1</sup>, GO exhibits higher constant phase element (CPE), which correlates to a rougher surface in this case.

The comparison of results from GO and rGO show the oxygen groups on the surface of GO play an important role in detection of lead ions. Although the electron transfer of GO in ferrocyanide is lower compared to normal SPEs and rGO electrodes, a higher current response with respect to lead ions is observed. After carrying out the optimization procedure, electrodes modified with 2 mg mL<sup>-1</sup> of GO were chosen. Various electrolytes were tested to find the optimal buffer for lead analysis. Two of the reagents, HCl and KCl, react very aggressively with the electrodes and destroy them. Another reagent, HNO<sub>3</sub>, has a large peak at -0.4 V that covers up the lead peak and makes detection of lead problematic, especially at low concentrations. Acetate (pH 5) exhibits better performance and lower background current than phosphate buffer solution (PBS pH 7) and as a result, 0.1 M acetate buffer with pH 5 was selected for measurement of lead concentrations.

## **B. Sensor Response in Lead Standard**

Square Wave Anodic Stripping Voltammetry (SWASV) has proven to be a powerful electrochemical method for sensing heavy metal ions. Taking that into consideration, SWASV was chosen as the preferred electrochemical method for this work and was optimized for the effects of accumulation potential, time, number of pulses, and the applied frequency.

Figure 4 indicates that when the pulse amplitude is increased to 50 mV, the peak current plateaus and subsequently remains steady as the pulse amplitude is increased. Additionally, the peak current response of GO SPE electrode was measured at different frequencies. It was observed that above 30 Hz, the peak splits into two peaks so that 20 Hz is optimal for the measurements. The peak current gradually increased with accumulation time until 240 s and a maximum peak current was obtained in deposition voltage of -1 V. However,

because of the over-potential involved during reduction of hydrogen on the surface of the electrodes, lower voltages are desirable for the purpose of long-term usage. As the application for this sensor is in situ measurement, all SWASV analyses have been done in stationary and ambient condition. The response under these conditions has enough sensitivity for lead detection at low concentrations. The cyclic voltammetry and differential pulse voltammetry of lead standard solution are shown in figure S3.

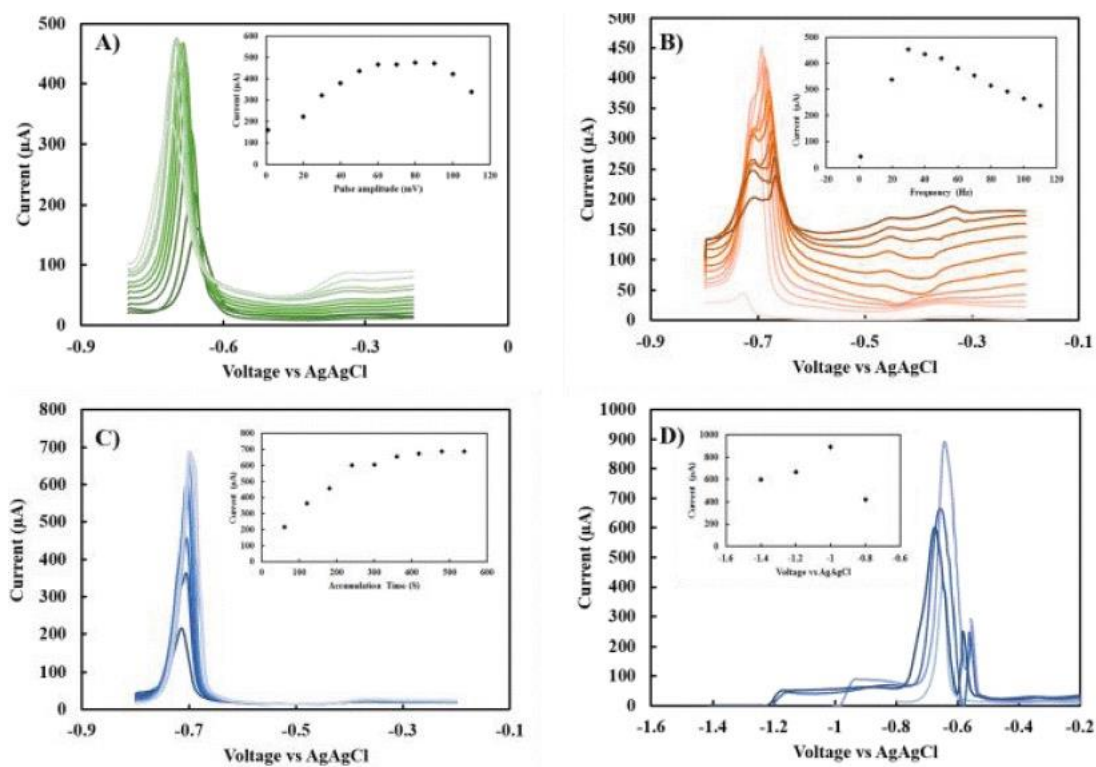


**Fig. 4.**

(A, B) Square wave anodic stripping voltammograms of different pulse amplitude, frequency, (C, D) accumulation time and accumulation voltage respectively. Lead concentration used was 20 ppm in 0.1 acetate buffer (pH 5).

After calibration of the SWASV parameters, the analytical performance of the lead GO-SPE was analyzed using SWASV. Figure 5A,B show SWASV measurements conducted from  $-0.85$  to  $-0.4$  V vs Ag/AgCl in acetate buffer (pH 5) for a wide range of lead ion concentrations (2 ppb–20 ppm). The peak current consistently appeared between  $-0.75$  V and  $-0.66$  V. At low concentration levels, which are the range of interest for sediment analysis, the

corresponding peak appeared at  $-0.75$  V. Figure 5C,D shows the calibration curves, indicating the presence of two linear ranges. The data has been corrected based on base line current. To calculate the sensitivity of the sensor, the effective surface area was obtained using the Randles-Sevcik equation:

$$i_p = 0.4463nFAC(nFvDRT)^{-1/2}$$

where,  $i_p$  is the maximum current in amps,  $n$  is the number of electrons involved in the redox reaction,  $A$  is the area of electrode,  $F$  is the Faraday constant,  $D$  is the diffusion constant,  $C$  is the concentration,  $v$  is the scan rate,  $R$  is the gas constant and  $T$  is the temperature. Based on the slope of the current versus the square root of the scan rate in  $5$  mM  $K_3Fe(CN)_6$  in  $0.1$  M KCl, the active surface area for spin coated  $2$  mg  $mL^{-1}$  of GO on top of the SPGE is equal to  $0.025$   $cm^2$ . On the basis of this area, the fabricated sensor shows a sensitivity of  $1.73$   $\mu A$   $ppb^{-1}$   $cm^{-2}$  in low and  $1.9$   $\mu A$   $ppb^{-1}$   $cm^{-2}$  in the high concentration range with a low detection limit of  $4$  ppb. The steady peaks in very high concentration levels indicate that the surface of GO is not saturated and the bond between oxygen functional group on the surface of GO with lead ions is reversible.

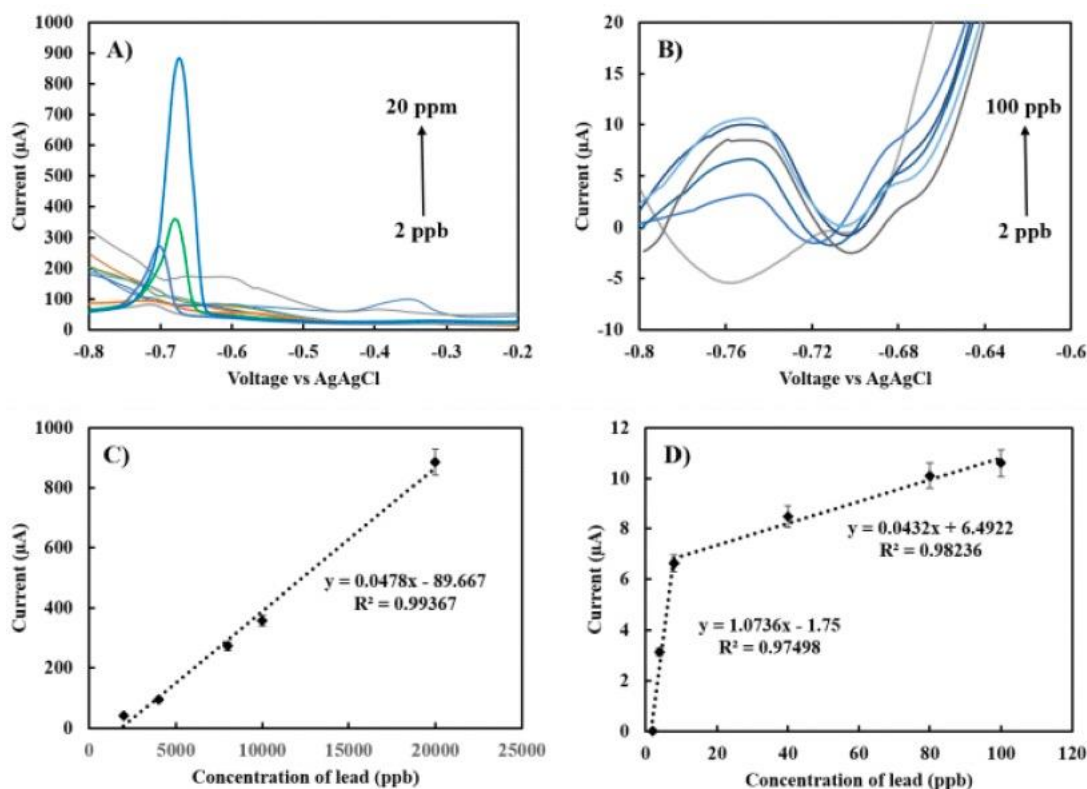


**Fig. 5.**

(A, B) Square wave anodic stripping voltammograms of different range of lead standard solution in acetate buffer (0–20 ppm). Pulse size is  $50$  mV, frequency  $20$  Hz, accumulation time  $240$  s. (C, D) Calibration curves for different concentration range of lead standard solutions.

Another challenge in the development of lead sensors is the selective determination of lead. The main interference is heavy metals and specifically cadmium and copper. The analytical performance of the sensor was investigated in presence of cadmium and copper ions standard solution. The results of this analysis are shown in figure S4.

### C. Lead Detection in Sediment Samples

After testing the performance of the fabricated sensor on lead standard solutions, the next step was to characterize the ability of the sensor to detect lead concentrations in contaminated complex environmental samples.

#### 1) Off-Chip Sample Preparation:

For measurement of basal concentrations of lead ions adsorbed to sediment, the sediment must first be digested with nitric acid to convert the various types of lead compounds to Pb (II). A sediment sample of 1000 mg (900 mg after water evaporation) was dispersed in nitric acid and then filtered using Whatman filter paper (Figure 6A). Ultrasonic agitation was used for 1 hour at 60° C in three different concentrations of nitric acid. Figure 6B shows the SWASV peaks for lead in a 1:1 ratio of digested sediment in nitric acid/acetate buffer. Among various concentrations, 0.1 M nitric acid was chosen based on peak current intensity and the need for a less aggressive solution on the electrode surface.

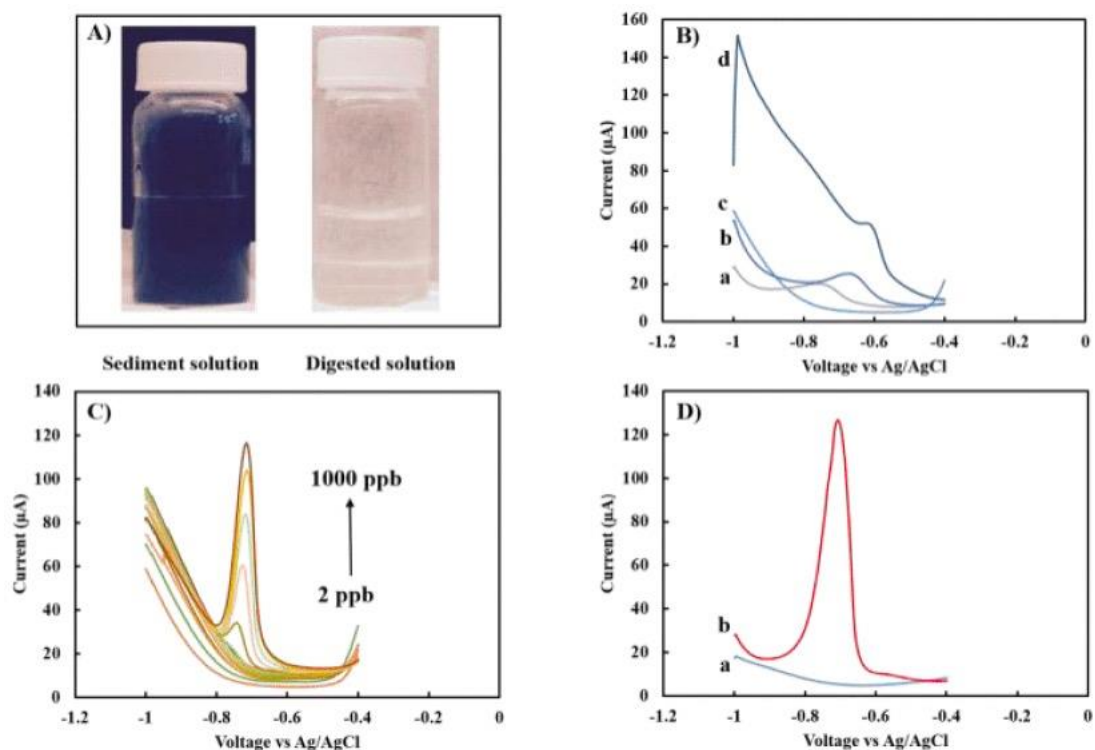




**Fig. 6.**

(A) Solution of sediment in nitric acid before and after filtration. (B) Effect of concentration of nitric acid using ultrasound digestion in 60 degrees a) digested in 0.1 M nitric acid, b) 0.2 M nitric acid. c) blank buffer solution 0.2 M nitric acid/acetate buffer, d) 0.3 M nitric acid (C) SWASV peaks for different concentration of lead standard solution in 1:1 nitric acid and acetate buffer. (D) SWASV peaks for a) 0.1 M nitric acid/acetate buffer blank, b) digested lead in 0.1 M nitric acid/acetate buffer.

To quantify the amount of lead, SWASV was performed for different lead standard solutions in the same electrolyte composition used for digestion (1:1 ratio 0.1 M nitric acid/acetate buffer). The results are shown in figure 6C. All digestions were performed at room temperature without ultrasonic agitation. Figure 6D shows the average result for three different measurements of samples with relative standard deviation (RSD) 10%. The peak intensity for the non-agitated sediments is significantly higher than for the agitated sediments, which was unexpected. This can be explained due to the sediment residues emerging during ultrasonication that can passivate the surface of the electrode. Based on the calibration data, the amount of lead in this sample is approximately  $21 \pm 2 \text{ mg kg}^{-1}$  of sediment, which is comparable with the range of lead in sediment reported in previous studies [1], [50].

### *2) Integration of Sample Preparation With Sensing Chip:*

After determining the appropriate reagents and conditions for sediment digestion, lead extraction, and purification, the final step was the miniaturization and integration of sample-preparation on-chip. First, a simple sponge was assembled on top of GO sensor. The detail of set up and the response of sensor is shown in figure S6. This initial result showed that integrated sample preparation was feasible, and the project moved towards an integrated fluidic system to minimize the need for operator expertise and manual injection of reagents.

To that end, the design was modified to incorporate precise microfluidic control to enable automation. In order to allow sufficient time for sediment digestion and to minimize user handling of reagents, a column was used to introduce sediment and nitric acid to the device (figure 7A). This design effectively decreases the volume of nitric acid required to the microliter range and reduces hazardous exposure for the user. In addition, the user is afforded more precise control of the ratio of reagents through separate inlet and outlet channels. The inlet configuration is as follows: The nitric acid inlet is located at the top of the column. The outlet is located in middle of the PDMS hole. The inlet of the acetate buffer is located on top of the hole. With this design, reagents are introduced at a (1:1) ratio to help obtain reproducible results

comparable to those obtained from calibration experiments. Figure 7B shows the result of the lead measurement obtained with this set up for 450 mg of dried sediment. Results are compared with traditional pretreatment methods (figure 7C, D).

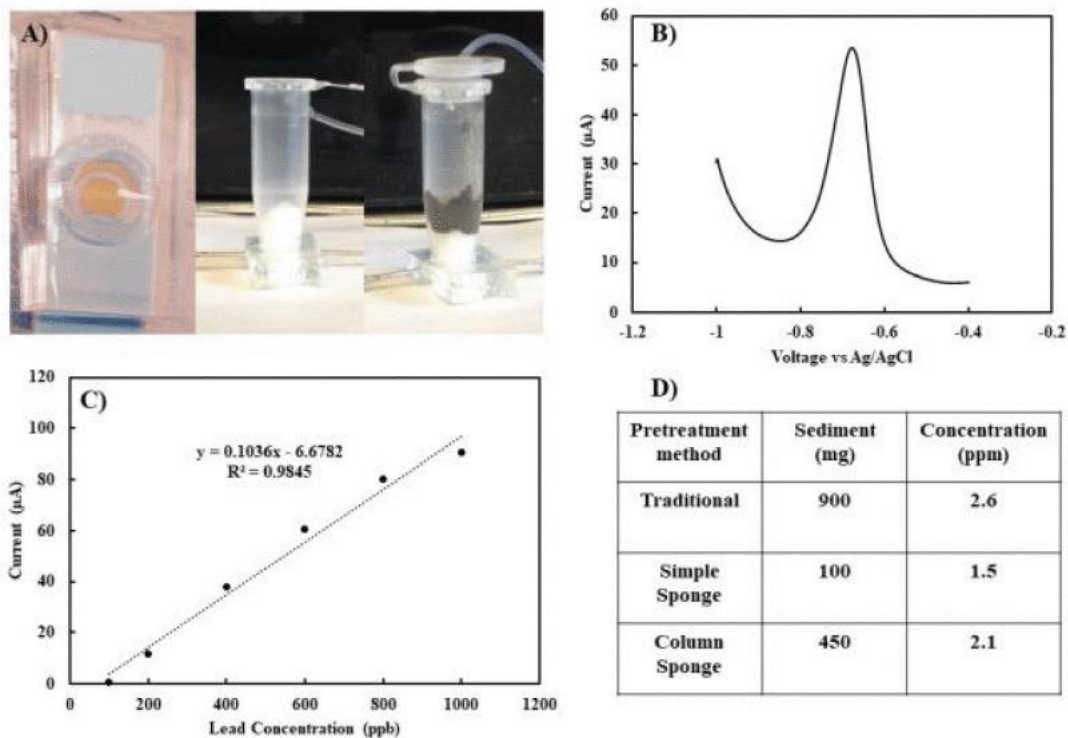


Fig. 7. (A) Column based pretreatment set up, (B) SWAVS response of column based compact electrochemical lead sensor, (C) Calibration curve for (1:1) nitric acid: acetate after baseline correction, (D) comparing results for different pretreatment approaches based on calibration curve.

## CONCLUSIONS

In this project, an integrated sample-to-answer platform was developed that is capable of analyzing heavy metal ions in complex samples like sediment. The results demonstrate that this approach shows promise for an in-situ platform capable of continuously monitoring heavy metal concentrations in complex environmental matrices such as sediment in natural water source. Although the focus of this work was sediment, this platform is applicable to perform sample-to-answer analysis in other complex matrices such as soil and

food [41], [42]. The approach presented in this manuscript uses a considerably shorter time for sediment digestion compared to off-chip pretreatment methods. Further improvement can be made to the design presented herein by incorporating a closed-feedback, loop-based input. This set up would allow the sediment to be exposed several times to the same volume of nitric acid, thus dramatically increasing the sensitivity.

An integrated miniaturized, sample-to-answer electrochemical sensor system based on graphene oxide was developed, calibrated and tested in both standard lead solutions and complex sediment samples. This work shows that square wave stripping voltammetry based electrochemical detection of lead is a promising analytical tool for monitoring heavy metals in complex matrices, and this work can fill the current gap for *in-situ* heavy metal monitoring using electrochemical based systems in natural water sources.

In this study, the outstanding electrochemical properties of graphene oxide thin films were utilized with respect to lead ions to fabricate a label-free method for measurement of low abundance toxic metals in sediment samples. The electrodes were systematically optimized for electrochemical measurement parameters in buffer solution, allowing measurement of lead at a low concentration. The sensitivity of the sensor was  $1.73 \mu\text{A ppb}^{-1} \text{cm}^{-2}$  in the range of 0–100 ppb and  $1.9 \mu\text{A ppb}^{-1} \text{cm}^{-2}$  in 100 ppb to 20 ppm with a low detection limit of 4 ppb. The performance of the sensor has been analyzed in both environmental samples spiked with lead (to test the effect of the matrix), and also with basal levels of lead in digested sediment. The final result is a portable pretreatment platform as an ultra-compact fully nitrated sample-to-answer system. This sensor shows the ability to quantify low abundance heavy metals in sediment. Further work includes miniaturizing the potentiostat used to readout the electrochemical sensor into a portable instrument resulting in a low-cost rapid field analyzer capable of sample-to-answer analysis simultaneously with collection of sediment. The full system can be used as an alternative to expensive and time-consuming methods such as atomic adsorption and inductively coupled plasma mass spectrometry.

## References

- [1] Z. Zhang, M. Li, W. Chen, S. Zhu, N. Liu, and L. Zhu, "Immobilization of lead and cadmium from aqueous solution and contaminated sediment using nano-hydroxyapatite," *Environ. Pollut.*, vol. 158, no. 2, pp. 514–519, Feb. 2010.

- [2] RTPN U.S. EPA National Center for Environmental Assessment. Air Quality Criteria for LEAD Final Report 2006. Accessed: Nov. 8, 2019. [Online]. Available: <https://cfpub.epa.gov/ncea/risk/recordisplay.cfm?deid=158823>
- [3] M. Ghaedi, A. Shokrollahi, K. Niknam, E. Niknam, S. Derki, and M. Soylak, "A cloud point extraction procedure for preconcentration/flame atomic absorption spectrometric determination of silver, zinc, and lead at subtrace levels in environmental samples," *J. AOAC Int.*, vol. 92, no. 3, pp. 907–913, May 2009.
- [4] D. Citak and M. Tuzen. (Aug. 2012). Cloud Point Extraction of Copper, Lead, Cadmium, and Iron Using 2,6-Diamino-4-Phenyl-1,3,5-Triazine and Nonionic Surfactant, and their Flame Atomic Absorption Spectrometric Determination in Water and Canned Food Samples. Accessed: Nov. 8, 2019. [Online]. Available: <https://www.ingentaconnect.com/content/aoac/jaoac/2012/00000095/00000004/art00029>
- [5] M. Soylak, E. Yilmaz, M. Ghaedi, M. Montazerzohori, and M. Sheibani. (Dec. 2012). Cloud Point Extraction and Flame Atomic Absorption Spectrometry Determination of Lead (II) in Environmental and Food Samples. Accessed: Nov. 8, 2019. [Online]. Available: <https://www.ingentaconnect.com/content/aoac/jaoac/2012/00000095/00000006/art00035>
- [6] R. Sitko, P. Janik, B. Feist, E. Talik, and A. Gagor, "Suspended aminosilanized graphene oxide nanosheets for selective preconcentration of lead ions and ultrasensitive determination by electrothermal atomic absorption spectrometry," *ACS Appl. Mater. Interfaces*, vol. 6, no. 22, pp. 20144–20153, Nov. 2014.
- [7] S. Caroli, G. Forte, A. L. Iamiceli, and B. Galoppi, "Determination of essential and potentially toxic trace elements in honey by inductively coupled plasma-based techniques," *Talanta*, vol. 50, no. 2, pp. 327–336, Sep. 1999. [8] S. Munro, L. Ebdon, and D. J. McWeeny, "Application of inductively coupled plasma mass spectrometry (ICP-MS) for trace metal determination in foods," *J. Anal. At. Spectrometry*, vol. 1, no. 3, pp. 211–219, Jan. 1986.
- [9] L. Zhao, S. Zhong, K. Fang, Z. Qian, and J. Chen, "Determination of cadmium(II), cobalt(II), nickel(II), lead(II), zinc(II), and copper(II) in water samples using dual-cloud point extraction and inductively coupled plasma emission spectrometry," *J. Hazardous Mater.*, vols. 239–240, pp. 206–212, Nov. 2012.
- [10] G. Pelosof, R. Tel-Vered, and I. Willner, "Amplified surface plasmon resonance and electrochemical detection of Pb<sup>2+</sup> ions using the Pb<sup>2+</sup>-dependent DNAzyme and hemin/G-quadruplex as a label," *Anal. Chem.*, vol. 84, no. 8, pp. 3703–3709, Apr. 2012.
- [11] A. Malon, T. Vigassy, E. Bakker, and E. Pretsch, "Potentiometry at trace levels in confined samples: Ion-selective electrodes with subfemtomole detection limits," *J. Amer. Chem. Soc.*, vol. 128, no. 25, pp. 8154–8155, Jun. 2006.
- [12] M.-R. Huang et al., "Synthesis of semiconducting polymer microparticles as solid ionophore with abundant complexing sites for longlife Pb(II) sensors," *ACS Appl. Mater. Interfaces*, vol. 6, no. 24, pp. 22096–22107, Dec. 2014.

- [13] S. J. R. Prabakar, C. Sakthivel, and S. S. Narayanan, "Hg(II) immobilized MWCNT graphite electrode for the anodic stripping voltammetric determination of lead and cadmium," *Talanta*, vol. 85, no. 1, pp. 290–297, Jul. 2011.
- [14] J. Li, S. Guo, Y. Zhai, and E. Wang, "High-sensitivity determination of lead and cadmium based on the nafion-graphene composite film," *Anal. Chim. Acta*, vol. 649, no. 2, pp. 196–201, Sep. 2009. [15] K. C. Armstrong, C. E. Tatum, R. N. Dansby-Sparks, J. Q. Chambers, and Z.-L. Xue, "Individual and simultaneous determination of lead, cadmium, and zinc by anodic stripping voltammetry at a bismuth bulk electrode," *Talanta*, vol. 82, no. 2, pp. 675–680, Jul. 2010.
- [16] J. L. Stauber and T. M. Florence, "The determination of trace metals in sweat by anodic stripping voltammetry," *Sci. Total Environ.*, vol. 60, pp. 263–271, Jan. 1987.
- [17] Z. Wang, G. Liu, L. Zhang, and H. Wang, "A bismuth modified hybrid binder carbon paste electrode for electrochemical stripping detection of trace heavy metals in soil," *Int. J. Electrochem. Sci.*, vol. 7, pp. 12326–12339, Dec. 2012.
- [18] Y. Wei et al., "SnO<sub>2</sub>/reduced graphene oxide nanocomposite for the simultaneous electrochemical detection of cadmium(II), lead(II), copper(II), and mercury(II): An interesting favorable mutual interference," *J. Phys. Chem. C*, vol. 116, no. 1, pp. 1034–1041, Jan. 2012.
- [19] L. Zhu, L. Xu, B. Huang, N. Jia, L. Tan, and S. Yao, "Simultaneous determination of Cd(II) and Pb(II) using square wave anodic stripping voltammetry at a gold nanoparticle-graphene-cysteine composite modified bismuth film electrode," *Electrochim. Acta*, vol. 115, pp. 471–477, Jan. 2014.
- [20] M. R. Mahmoudian, Y. Alias, W. J. Basirun, P. M. Woi, M. Sookhakian, and F. Jamali-Sheini, "Synthesis and characterization of Fe<sub>3</sub>O<sub>4</sub> rose like and spherical/reduced graphene oxide nanosheet composites for lead (II) sensor," *Electrochim. Acta*, vol. 169, pp. 126–133, Jul. 2015.
- [21] J. Zhuang, L. Fu, M. Xu, Q. Zhou, G. Chen, and D. Tang, "DNAzymebased magneto-controlled electronic switch for picomolar detection of lead (II) coupling with DNA-based hybridization chain reaction," *Biosensors Bioelectron.*, vol. 45, pp. 52–57, Jul. 2013. [22] S. Tang, P. Tong, H. Li, J. Tang, and L. Zhang, "Ultrasensitive electrochemical detection of Pb<sup>2+</sup> based on rolling circle amplification and quantum dotstaggng," *Biosensors Bioelectron.*, vol. 42, pp. 608–611, Apr. 2013.
- [23] R. Seenivasan, W.-J. Chang, and S. Gunasekaran, "Highly sensitive detection and removal of lead ions in water using cysteine-functionalized graphene oxide/polypyrrole nanocomposite film electrode," *ACS Appl. Mater. Interfaces*, vol. 7, no. 29, pp. 15935–15943, Jul. 2015.
- [24] J.-T. Zhang, Z.-Y. Jin, W.-C. Li, W. Dong, and A.-H. Lu, "Graphene modified carbon nanosheets for electrochemical detection of Pb(II) in water," *J. Mater. Chem. A*, vol. 1, no. 42, pp. 13139–13145, Oct. 2013.

- [25] C. Gao, X.-Y. Yu, R.-X. Xu, J.-H. Liu, and X.-J. Huang, "AlOOH-reduced graphene oxide nanocomposites: One-pot hydrothermal synthesis and their enhanced electrochemical activity for heavy metal ions," *ACS Appl. Mater. Interfaces*, vol. 4, no. 9, pp. 4672–4682, Sep. 2012.
- [26] N. Promphet, P. Rattanarat, R. Rangkupan, O. Chailapakul, and N. Rodthongkum, "An electrochemical sensor based on graphene/polyaniline/polystyrene nanoporous fibers modified electrode for simultaneous determination of lead and cadmium," *Sens. Actuators B, Chem.*, vol. 207, pp. 526–534, Feb. 2015.
- [27] G. Aragay, J. Pons, and A. Merkoçi, "Recent trends in macro-, micro-, and nanomaterial-based tools and strategies for heavy-metal detection," *Chem. Rev.*, vol. 111, no. 5, pp. 3433–3458, May 2011. [28] D. Cai and M. Song, "Preparation of fully exfoliated graphite oxide nanoplatelets in organic solvents," *J. Mater. Chem.*, vol. 17, no. 35, pp. 3678–3680, Aug. 2007.
- [29] X. Wang, L. Zhi, and K. Müllen, "Transparent, conductive graphene electrodes for dye-sensitized solar cells," *Nano Lett.*, vol. 8, no. 1, pp. 323–327, Jan. 2008.
- [30] L. J. Cote, F. Kim, and J. Huang, "Langmuir–Blodgett assembly of graphite oxide single layers," *J. Amer. Chem. Soc.*, vol. 131, no. 3, pp. 1043–1049, Jan. 2009.
- [31] G. Eda, G. Fanchini, and M. Chhowalla, "Large-area ultrathin films of reduced graphene oxide as a transparent and flexible electronic material," *Nature Nanotechnol.*, vol. 3, no. 5, pp. 270–274, May 2008.
- [32] J. T. Robinson et al., "Wafer-scale reduced graphene oxide films for nanomechanical devices," *Nano Lett.*, vol. 8, no. 10, pp. 3441–3445, Oct. 2008.
- [33] J. T. Robinson, F. K. Perkins, E. S. Snow, Z. Wei, and P. E. Sheehan, "Reduced graphene oxide molecular sensors," *Nano Lett.*, vol. 8, no. 10, pp. 3137–3140, Oct. 2008.
- [34] S. Pang, H. N. Tsao, X. Feng, and K. Müllen, "Patterned graphene electrodes from solution-processed graphite oxide films for organic field-effect transistors," *Adv. Mater.*, vol. 21, no. 34, pp. 3488–3491, Sep. 2009.
- [35] Z. Wang, H. Wang, Z. Zhang, and G. Liu, "Electrochemical determination of lead and cadmium in rice by a disposable bismuth/electrochemically reduced graphene/ionic liquid composite modified screen-printed electrode," *Sens. Actuators B, Chem.*, vol. 199, pp. 7–14, Aug. 2014.
- [36] J.-M. Jian, Y.-Y. Liu, Y.-L. Zhang, X.-S. Guo, and Q. Cai, "Fast and sensitive detection of Pb<sup>2+</sup> in foods using disposable screen-printed electrode modified by reduced graphene oxide," *Sensors*, vol. 13, no. 10, pp. 13063–13075, Sep. 2013.

## RECOMMENDATIONS

This platform developed has great promise for having a high impact for society.